Molecular-Atomic Transition along the Deuterium Hugoniot Curve with Coupled Electron-Ion Monte Carlo Simulations

Norm M. Tubman,[1,*] Elisa Liberatore,[2] Carlo Pierleoni,[3] Markus Holzmann,[4] and David M. Ceperley[1]
[1]Department of Physics, University of Illinois, Urbana, Illinois 61801, USA
[2]EPFL, Route Cantonale, 1015 Lausanne, Switzerland
[3]Department of Physical and Chemical Sciences, University of L'Aquila and CNISM UdR L'Aquila, Via Vetoio 10, I-67010 L'Aquila, Italy
[4]LPTMC, Université Pierre et Marie Curie and CNRS, 75005 Paris, France and LPMMC, Université Grenoble I and CNRS, 38042 Grenoble, France
(Received 21 August 2014; published 22 July 2015)

We have performed simulations of the principal deuterium Hugoniot curve using coupled electron-ion Monte Carlo calculations. Using highly accurate quantum Monte Carlo methods for the electrons, we study the region of maximum compression along the Hugoniot, where the system undergoes a continuous transition from a molecular fluid to a monatomic fluid. We include all relevant physical corrections so that a direct comparison to experiment can be made. Around 50 GPa we find a maximum compression of 4.85. This compression is approximately 5.5% higher than previous theoretical predictions and 15% higher than the most accurate experimental data. Thus first-principles simulations encompassing the most advanced techniques are in disagreement with the results of the best experiments.

DOI: 10.1103/PhysRevLett.115.045301 PACS numbers: 67.63.Cd, 64.30.-t, 71.15.Mb

The study of high pressure hydrogen is particularly interesting as progress in the field has come about from difficult experiments under extreme conditions and computationally expensive quantum simulations [1]. Experiments on hydrogen under high pressure have direct implications for planetary science: laboratory setups attempt to recreate the extreme conditions which describe planetary formation and equilibrium properties of planetary interiors [2–6]. Improvements from both theory and experiment have been essential to creating our current understanding of the hydrogen phase diagram [7–10]. A key experimental technique to probe hydrogen under extreme conditions is dynamic compression via shock wave generation. The principal Hugoniot [9–12] is determined by shocking a material from an initial state to a state of higher pressure, temperature, and density. The locus of points reachable in such an experiment, the so-called Hugoniot, is determined by conservation laws and initial conditions. Shock experiments often use deuterium instead of hydrogen, because of its higher number density at ambient pressure, in order to reach higher density of the shocked state [13–22]. Theoretical methods used so far to investigate this interesting region of phase diagram are based on density functional theory (DFT) which is expected to describe molecular dissociation and metallization with only limited accuracy. In this work we present highly accurate quantum Monte Carlo (QMC) results for the crossover between the molecular liquid to monatomic liquid along the principal deuterium Hugoniot. We find that the maximum compression at the molecular dissociation crossover is 5.5% larger than previous predictions from DFT.

Among the computational methods used in electronic structure simulations, QMC simulations are considered among the highest quality [23–26], with the fixed-node quantum Monte Carlo (FNQMC) method being the most accurate [27–34]. The coupled electron ion Monte Carlo (CEIMC) method [35–37] uses FNQMC to determine the electronic ground state energy. The ionic coordinates are then sampled at a finite temperature from the Boltzmann distribution using the Born-Oppenheimer energy surface [38–40] determined by FNQMC. We use variational Monte Carlo (VMC) calculations with DFT orbitals in the electronic trial wave function, path integral Monte Carlo (PIMC) calculations to account for the zero point motion of the ions [41,42], correlated sampling for calculating energy differences [43], and the reptation quantum Monte Carlo (RQMC) method for calculating unbiased estimators in FNQMC [28].

Deuterium Hugoniot function.—Shock experiments are used to determine the equation of state of a material that is in an initial state at a known energy, pressure, and volume (E_0, P_0, v_0). The zeros of the Hugoniot function $H(v,T)$ determine the final conditions E, P, v as

$$H(v,T) = e(v,T) - e_0 + \frac{1}{2}(v - v_0)[P(v,T) + P_0] = 0, \quad (1)$$

where v is the atomic volume, $e(v,T)$ is the internal energy per atom and $P(v,T)$ is the pressure. We assume initial conditions (0.167 g/cm^3, 22 K, 1.24×10^{-4} GPa) in order to compare directly with some of the previous experiments [13]. We estimated the initial energy to be $e_0 = -0.583725$ Ha/atom from the energy of an isolated D_2 molecule [44], the estimated low temperature binding energy of solid D_2 [45], and integration of the heat capacity [46]. The difference between the principal Hugoniot for

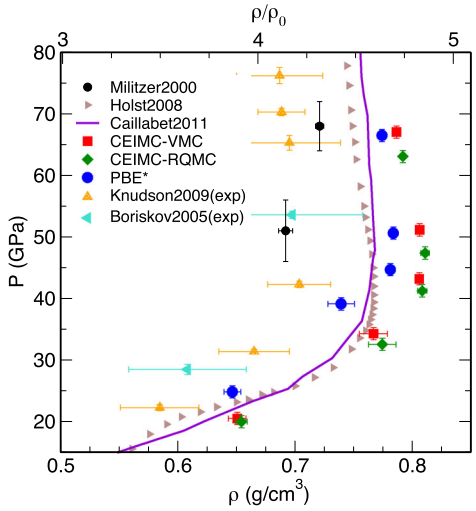

FIG. 1 (color online). The principal deuterium Hugoniot compared to previous theoretical and experimental studies. Holst [47] and Caillabet [48] are DFT-PBE simulations, Militzer [49] is a PIMC simulation. The PBE* results are generated by solving the Hugoniot equation using the CEIMC-VMC configurations but computing energy and pressure with DFT-PBE. Knudson [22] and Boriskov [14] are experimental results. The initial density for the Boriskov experiment was $\rho_0 = 0.171$ g/cm^3, slightly higher than for the other Hugoniots. The value $\rho_0 = 0.167$ g/cm^3 has been used in computing the upper relative compression scale.

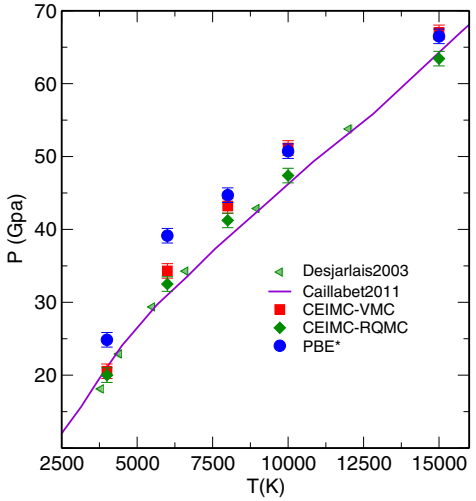

FIG. 2 (color online). Pressure vs temperature along the deuterium Hugoniot compared to previous theoretical studies.

deuterium and hydrogen comes about primarily because of the differing initial conditions. In this Letter, we use atomic units for energies, GPa for pressures, and r_s units for density where $4\pi r_s^3/3 = 1/n$ with n is the electron number density in atomic units. The initial density corresponds to $r_s = 3.184$.

To calculate the Hugoniot in the region of interest, we perform simulations in the range of $1.80 \le r_s \le 2.00$ and 4000 K $\le T \le$ 15 000 K. Fitting $H(v, T)$ at fixed T to a quadratic polynomial in r_s we solve for $H = 0$. Our results are shown in Figs. 1 and 2 and Table I. The main result is the CEIMC-RQMC curve. The predictions labeled by CEIMC-VMC and PBE* are also from this work and will be discussed later.

Previous theoretical results have been generated from a variety of different methods which include DFT, PIMC, and wave packet MD [47–55]. Hugoniot curves have been calculated using DFT with the PBE functional [56]; several of them are shown in Figs. 1 and 2 (Holst2008 [47], Caillabet2011 [48], and Desjarlais2003 [50]). The DFT studies generally show similar behavior when compared with each other, but other methods that involve different approximations generally do not agree with these results, especially in the crossover region. For instance, previous restricted-PIMC calculations [49] with variational density matrix nodes have significantly different behavior.

There are notable differences between previous DFT predictions and our results. The DFT Hugoniot curves consistently show a maximum compression of ~4.60, but the CEIMC results show a maximum compression of ~4.85. It might be expected that most DFT functionals would struggle to capture the physics of this crossover, as the energies of bond breaking of just two hydrogen atoms (or deuterium atoms) are poorly described with many density functionals such as PBE. However, it is not clear that this is the origin of the discrepancy since the average distance between hydrogen atoms at these pressures is smaller than needed to break the hydrogen bond.

There has been extensive experimental work in measuring the Hugoniot for deuterium [13–22,57–59] and hydrogen [59–63]. Experimental data from Refs. [14,22] are plotted for the Hugoniot in Fig. 1. The CEIMC, Knudson, and Caillabet results all suggest a maximum compression at 40 GPa, whereas the Militzer and Boriskov data suggest a maximum compression above 100 GPa. The experimental results disagree with our Hugoniot points by three standard deviations at temperatures 8 and 10 K, in the region of maximum compression. Overall the experimental results are systematically less compressed than our theoretical prediction. Since we believe our theoretical results take into account all relevant sources of error, this suggests there are some systematic errors in the experimental results.

TABLE I. CEIMC-RQMC estimates of the principal Hugoniot: Pressures, r_s, deuterium mass density, compression, and temperature.

P (GPa)	r_s	ρ_d (g/cm^3)	ρ_d/ρ_0	T (10^3 K)
18(1)	2.019(5)	0.654(5)	3.91(3)	4
32(1)	1.909(9)	0.773(9)	4.63(6)	6
39(1)	1.882(3)	0.807(4)	4.83(2)	8
48(1)	1.880(3)	0.810(4)	4.85(2)	10
66(1)	1.895(1)	0.791(2)	4.73(1)	15

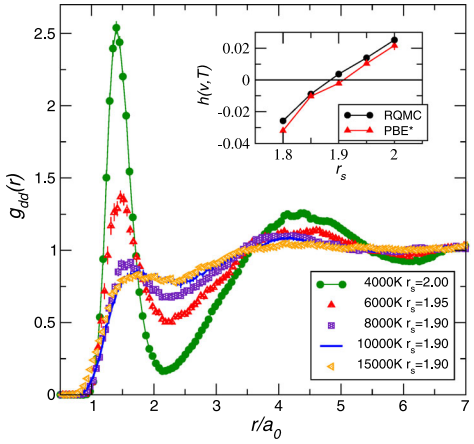

FIG. 3 (color online). Ion-ion radial distribution function $g_{dd}(r)$, near the Hugoniot line. The large peak for $1 < r < 2$ signals the presence of bonded atoms and indicates the majority of the atoms are bound into molecules at 4000 K. This peak nearly disappears as the system becomes a monatomic liquid at 8000 K, although a small feature remains. The ion-ion distribution function at $T = 10\,000$ K overlaps almost entirely with the $T = 15\,000$ K curve. Inset: The Hugoniot function plotted at 8000 K, for CEIMC-RQMC and DFT-PBE.

Evidence of the bond-breaking crossover is given in Fig. 3 where we present the radial distribution function between ions along the Hugoniot. The minimum temperature at which we observe the breaking of molecules is density dependent. At the highest density in this work $r_s = 1.80$, a small increase in the temperature over 4000 K causes a transition to the monatomic phase whereas in the lowest density systems $r_s = 2.00$, the crossover does not occur until the system is above 10 000 K. Using our PBE* results (the details are discussed below), we see a closing of the electronic band gap in going from 6000 to 8000 K along the Hugoniot curve, signaling what is likely to be a continuous crossover to a metallic state [47].

Method.—We now discuss the details of the method used in the simulations. It is crucial that the QMC electronic structure calculations are performed with accurate trial wave functions. These have a single Slater determinant for each spin component and a correlation part with single, two, and three body Jastrows. We use DFT-PBE Kohn-Sham orbitals in the Slater determinants [64]. They are recalculated as the ions move. The backflow transformation is applied to those orbitals. Analytical expressions from the random phase approximation (RPA) for both correlation and backflow functions are employed [35,65–67] which exactly enforce the cusp conditions between all pairs of charges as well as the correct long-wavelength behavior of the charge oscillations. These are complemented by empirical expressions, with a few variational parameters [35,66]. To mitigate the computational effort we optimize the wave function parameters over an ensemble of statistically independent configurations at thermal equilibrium for each given density. We find that using this form of the wave function yields energies within 1 mHa/atom of a full optimization of each configuration individually.

Our simulations consist of 54 ions and 54 electrons at fixed volume and temperature. CEIMC runs are performed with energy differences from VMC. To demonstrate the quality of our wave function we select statistically independent configurations generated during the CEIMC run and compare VMC with RQMC energies, as shown in Table II.

In order to calculate an accurate Hugoniot the errors in the energy and pressure need to be consistent across densities for a given temperature. This consistency is apparent in our data for all the temperatures considered in this work. Just as important, the largest discrepancy is less than 1 mHa/atom, which is small enough as to not influence the results more than the final error bars on our calculated Hugoniot curves.

Also we report relative energy errors in Table II. The relative energies between configurations is an indicator of whether we are sampling an accurate thermal distribution for the ions. Table II shows that these relative energy differences are significantly less than 1 mHa/atom. To test the quality of our sampled distribution, we used reweighting [68] at 8000 K for $r_s = 1.85$, 1.90 over 1500 nuclear configurations. This resulted in an efficiency of 0.5 which suggests a large enough overlap between the RQMC-generated and VMC-generated ionic distributions to trust the results.

Approximations and corrections.—Because of the nature of these simulations, several other approximations enter beyond the electronic structure. Single particle finite size effects can be accounted for by using twisted boundary conditions [69]. We used a fixed grid of $(4 \times 4 \times 4)$ twisted angles. The many body finite size effects can be estimated [70–72] by extrapolating the small wavelength limit of the charge-charge structure factor $S_{qq}(k)$. The corrections comprise a kinetic energy contribution, $\Delta K = 3/\sqrt{16 r_s^3}$, and a potential energy contribution

TABLE II. Energy differences (mHa/atom) between CEIMC-RQMC and CEIMC-VMC at various densities and temperatures. The "Avg Err" is the mean absolute error (MAE) of the energies over configurations, and "Rel Err" is the MAE between configurations after the energies have been shifted by the average energy difference of the entire set. Configurations are sampled with CEIMC-VMC; the CEIMC-RQMC energy differences are calculated from a set of 100 configurations.

Avg Err	r_s	4000 (K)	6000	8000	10 000	15 000
	1.8	2.7(3)	3.2(3)	3.4(3)	3.6(3)	4.1(3)
	1.85	3.0(3)	3.2(3)	3.6(3)	3.8(3)	4.5(3)
	1.9	3.2(3)	3.5(3)	3.9(3)	4.5(3)	4.6(3)
Rel Err	r_s	4000 (K)	6000	8000	10 000	15 000
	1.8	0.16(1)	0.21(2)	0.27(2)	0.34(3)	0.42(3)
	1.85	0.18(2)	0.22(2)	0.19(2)	0.32(2)	0.48(3)
	1.9	0.16(2)	0.24(3)	0.28(5)	0.33(5)	0.44(4)

TABLE III. Pressure errors of VMC and PBE estimated using RQMC. Configurations are sampled with CEIMC-VMC and the PBE* and RQMC pressure differences are calculated from them. Shown are MAE in GPa. The unit KK stands for 10^3 K.

r_s	8 KK-VMC	10KK-VMC	8KK-PBE*	10KK-PBE*
1.8	2.8(2)	2.8(2)	6.4(2)	6.3(2)
1.85	2.3(2)	2.7(2)	3.1(2)	3.7(2)
1.9	2.7(2)	3.6(2)	6.1(3)	5.7(3)

TABLE IV. Energy errors of VMC and PBE estimated using RQMC. Configurations are sampled with CEIMC-VMC and the PBE* and RQMC energy differences are calculated from them. Shown are MAE in mHa/atom. The unit KK stands for 10^3 Kelvin.

r_s	8 KK-VMC	10 KK-VMC	8 KK-PBE*	10 KK-PBE*
1.8	3.4(3)	3.6(3)	4.0(3)	3.7(3)
1.85	3.6(3)	3.8(3)	3.6(3)	4.2(3)
1.9	3.9(3)	4.5(3)	4.2(3)	3.5(3)

$\Delta V = 3r_s^{-3}\lim_{k\to 0}[S_{qq}(k)/k^2]$. Corrections to the pressure are accounted for using the virial expression [73], $\Delta P = [(2\Delta K + \Delta V)\rho]/3$.

Corrections from electronic thermal effects are estimated using DFT-PBE. Given a set of representative configurations from CEIMC, we computed the DFT energy with a smearing of the electronic density over an ensemble of single particle orbitals weighted by the Fermi-Dirac distribution. Once the energies and pressures have been calculated in DFT, there are two types of corrections that could be applied. First, the thermal DFT energy and pressure corrections can be added in directly to correct our QMC energies and pressures. We calculated these effects on 50 configurations for each temperature or density considered in this work and observed no effect within our error bars. The second correction involves reweighting the configurations with the electronic entropy term to incorporate the effects of using the Mermin finite temperature functional [74]. We tested this at 8000 K and observed no effect within our error bars. It is not clear whether including these thermal corrections improves our estimates, as both the DFT band gaps and pressures are important in determining thermal effects. The problems with DFT band gaps are well studied [75–78], and below we show that the DFT pressure errors are significant.

Nuclear quantum effects can be explicitly taken into account in CEIMC by replacing the "classical" charge with a dynamic deuteron using PIMC for the deuterons. Note that at the temperature of this study it is not necessary to consider the effect of the deuteron's spin. We consider the deuterons as distinguishable quantum particles. However, because the temperatures considered here are high and such calculations are computationally more expensive, we did such PIMC simulations at only two densities ($r_s = 1.80, 2.00$) and at $T = 8000$ K. We found no effect on the energies and pressures within our error bars. Further, we have estimated the nuclear quantum effects at $T = 4000$ K using the molecular zero point energy $\hbar\omega_0/2$ with ω_0 fitted to the observed bond distribution [47]. Corrections to the energy and pressure are significant at this lower temperature but the global effect on the Hugoniot is within the error bars.

To increase the accuracy of our predictions, we add in the RQMC energy and pressure as a correction to our CEIMC-VMC results. RQMC calculations of the energy and pressure are extrapolated to infinite projection time (β) and zero time step ($\Delta\tau$).

Finally, we describe a test we used to determine the origin of the differences between the DFT-PBE and CEIMC simulations. The CEIMC simulations use a VMC calculation of the energy to generate configurations. We use these configurations to identify how the DFT-PBE functional behaves differently from QMC, keeping the finite size corrections and the thermal corrections fixed. PBE calculations were performed without any pseudopotential but with a sufficiently high plane wave cutoff (500 Ry) to converge the energies and pressures. The PBE calculations were done at zero temperature with the same k-point sampling used for our QMC twist averaging. With this data we recalculated the Hugoniot. The results are shown in the Figs. 1 and 2 as PBE*. We are most interested in the temperatures at 8000 and 10 000 K where our CEIMC calculations exhibit the largest compression. The PBE* curve at both these temperatures is less compressed (4.6), than our VMC/RQMC results. We can understand this result by considering the energy and pressure errors in Tables III and IV. The VMC and PBE* energy errors are actually quite close, and consistently agree within error bars for this part of the phase diagram. A trace of the energies for the individual configurations suggests that the two methods generate very similar, though not identical, ionic configurations. The change in the PBE* curve mainly comes from errors in the pressure as shown in Table III. These pressure errors are in many cases more than twice as large as the VMC and their magnitude fluctuates significantly at different densities. This is in comparison to the VMC pressure errors which are not only smaller, but also consistent with the energy errors giving similar values for the VMC and RQMC Hugoniot functions. A comparison of PBE* and the RQMC Hugoniot functions is plotted in the inset of Fig. 3.

Discussion and conclusions.—In this work we have performed a calculation along the principal Hugoniot of deuterium as the molecular fluid transforms into monoatomic fluid. Our results show that deuterium is more compressible than estimated on the basis of previous DFT-PBE simulations. A large part of the difference arises from errors in the DFT pressures, and both energy and pressure errors become more significant at temperatures

below 8000 K. This represents one of the first works for dense deuterium in which all the relevant physical effects were taken into account without the possibility for any large uncontrolled errors. Our results suggest that there are systematic errors in the experimental results that remain to be resolved in future experiments.

We thank L. Schulenburger, L. Benedict, W. Nellis, E. Brown, T. Mattsson, H. Changlani, I. Kylanpaa, and M. Knudson for useful discussions. This work was supported by DOE DE-NA0001789. C. P. was supported by the Italian Institute of Technology (IIT) under the SEED project Grant No. 259 SIMBEDD. M. H. was supported by the Fondation Nanosiences de Grenoble. Computer time was provided by XSEDE, supported by the National Science Foundation Grant No. OCI-1053575, and by PRACE Projects No. 2011050781 and No. 2013091918.

*normantubman2015@u.northwestern.edu

[1] J. M. McMahon, M. A. Morales, C. Pierleoni, and D. M. Ceperley, Rev. Mod. Phys. **84**, 1607 (2012).
[2] D. J. Stevenson, Annu. Rev. Earth Planet Sci. **10**, 257 (1982).
[3] B. Militzer, W. B. Hubbard, J. Vorberger, I. Tamblyn, and S. A. Bonev, Astrophys. J. Lett. **45**, 688 (2008).
[4] N. Nettelmann, B. Holst, A. Kietzmann, M. French, R. Redmer, and D. Blaschke, Astrophys. J. **683**, 1217 (2008).
[5] T. Guillot, Annu. Rev. Earth Planet Sci. **33**, 493 (2005).
[6] J. Fortney, Science **305**, 1414 (2004).
[7] J. Vorberger, I. Tamblyn, B. Militzer, and S. A. Bonev, Phys. Rev. B **75**, 024206 (2007).
[8] M. A. Morales, C. Pierleoni, E. Schwegler, and D. M. Ceperley, Proc. Natl. Acad. Sci. U.S.A. **107**, 12799 (2010).
[9] W. Nellis, Rep. Prog. Phys. **69**, 1479 (2006).
[10] M. Ross, Rep. Prog. Phys. **48**, 1 (1985).
[11] W. J. M. Rankine, Phil. Trans. R. Soc. London **160**, 277 (1870).
[12] J. N. Johnson and R. Cheret, *Classic Papers in Shock Compression Science*, 1st. ed. (Springer, New York, 1998).
[13] M. D. Knudson, D. L. Hanson, J. E. Bailey, C. A. Hall, J. R. Asay, and C. Deeney, Phys. Rev. B **69**, 144209 (2004).
[14] G. V. Boriskov, A. I. Bykov, R. I. Il'kaev, V. D. Selemir, G. V. Simakov, R. F. Trunin, V. D. Urlin, A. N. Shuikin, and W. J. Nellis, Phys. Rev. B **71**, 092104 (2005).
[15] W. J. Nellis, Phys. Rev. Lett. **89**, 165502 (2002).
[16] D. G. Hicks, T. R. Boegly, P. M. Celliers, J. H. Eggert, S. J. Moon, D. D. Meyerhofer, and G. W. Collins, Phys. Rev. B **79**, 014112 (2009).
[17] S. Grishechkin, S. Gruzdev, V. Gryaznov, M. Zhernokletov, R. Il'Kaev, I. Iosilevskii, G. Kashintseva, S. Kirshanov, S. Manachkin, and V. Mintsev, JETP Lett. **80**, 398 (2004).
[18] S. Belov, G. Boriskov, A. Bykov, R. Il'Kaev, N. Luk'yanov, A. Matveev, O. Mikhailova, V. Selemir, G. Simakov, and R. Trunin, JETP Lett. **76**, 433 (2002).
[19] C. Wang, X. He, and P. Zhang, J. Appl. Phys. **108**, 044909 (2010).
[20] M. van Thiel, M. Ross, B. Hord, A. Mitchell, W. Gust, M. D'Addario, R. Keeler, and K. Boutwell, Phys. Rev. Lett. **31**, 979 (1973).
[21] M. D. Knudson, D. L. Hanson, J. E. Bailey, C. A. Hall, and J. R. Asay, Phys. Rev. Lett. **90**, 035505 (2003).
[22] M. D. Knudson and M. P. Desjarlais, Phys. Rev. Lett. **103**, 225501 (2009).
[23] J. C. Grossman, J. Chem. Phys. **117**, 1434 (2002).
[24] N. M. Tubman, J. L. DuBois, R. Q. Hood, and B. J. Alder, J. Chem. Phys. **135**, 184109 (2011).
[25] N. M. Tubman, J. L. DuBois, and B. J. Alder, in *Advances in Quantum Monte Carlo*, ACS Symposium Series Vol. 1094 (ACS, Washington, DC, 2012), Chap. 5, pp. 41–50.
[26] E. Neuscamman, J. Chem. Phys. **139**, 194105 (2013).
[27] W. M. C. Foulkes, L. Mitas, R. J. Needs, and G. Rajagopal, Rev. Mod. Phys. **73**, 33 (2001).
[28] S. Baroni and S. Moroni, Phys. Rev. Lett. **82**, 4745 (1999).
[29] L. Shulenburger and T. R. Mattsson, Phys. Rev. B **88**, 245117 (2013).
[30] R. C. Clay, J. Mcminis, J. M. McMahon, C. Pierleoni, D. M. Ceperley, and M. A. Morales, Phys. Rev. B **89**, 184106 (2014).
[31] J. T. Krogel, J. Kim, and F. A. Reboredo, Phys. Rev. B **90**, 035125 (2014).
[32] H. Zheng and L. K. Wagner, Phys. Rev. Lett. **114**, 176401 (2015).
[33] K. Foyevtsova, J. T. Krogel, J. Kim, P. R. C. Kent, E. Dagotto, and F. A. Reboredo, Phys. Rev. X **4**, 031003 (2014).
[34] S. Azadi, B. Monserrat, W. M. C. Foulkes, and R. J. Needs, Phys. Rev. Lett. **112**, 165501 (2014).
[35] D. Ceperley, M. Dewing, and C. Pierleoni, in *Bridging Time Scales: Molecular Simulations for the Next Decade*, Lecture Notes in Physics Vol. 605, edited by P. Nielaba, M. Mareschal, and G. Ciccotti (Springer-Verlag, Berlin, 2002), p. 473.
[36] D. M. Ceperley and M. Dewing, J. Chem. Phys. **110**, 9812 (1999).
[37] C. Pierleoni and D. M. Ceperley, Lect. Notes Phys. **714**, 641 (2006).
[38] M. Born and J. Oppenheimer, Ann. Phys. (Berlin) **389**, 457 (1927).
[39] N. M. Tubman, I. Kylänpää, S. Hammes-Schiffer, and D. M. Ceperley, Phys. Rev. A **90**, 042507 (2014).
[40] J. Mitroy, S. Bubin, W. Horiuchi, Y. Suzuki, L. Adamowicz, W. Cencek, K. Szalewicz, J. Komasa, D. Blume, and K. Varga, Rev. Mod. Phys. **85**, 693 (2013).
[41] D. M. Ceperley, Rev. Mod. Phys. **67**, 279 (1995).
[42] D. M. Ceperley, in *Monte Carlo and Molecular Dynamics of Condensed Matter Systems*, edited by K. Binder and G. Ciccotti (Editrice Compositori, Bologna, 1996).
[43] B. L. Hammond, P. J. Reynolds, and W. A. Lester, *Monte Carlo Methods in Ab Initio Quantum Chemistry* (World Scientific, Singapore, 1994).
[44] W. Kolos and L. Wolniewicz, J. Chem. Phys. **41**, 3674 (1964).
[45] I. F. Silvera, Rev. Mod. Phys. **52**, 393 (1980).
[46] P. C. Sauers, *Hydrogen Properties for Fusion Energy* (University of California Press, Berkeley, 1986).

[47] B. Holst, R. Redmer, and M. P. Desjarlais, Phys. Rev. B **77**, 184201 (2008).
[48] L. Caillabet, S. Mazevet, and P. Loubeyre, Phys. Rev. B **83**, 094101 (2011).
[49] B. Militzer and D. M. Ceperley, Phys. Rev. Lett. **85**, 1890 (2000).
[50] M. P. Desjarlais, Phys. Rev. B **68**, 064204 (2003).
[51] V. S. Filinov, M. Bonitz, W. Ebeling, and V. E. Fortov, Plasma Phys. Controlled Fusion **43**, 743 (2001).
[52] T. J. Lenosky, S. R. Bickham, J. D. Kress, and L. A. Collins, Phys. Rev. B **61**, 1 (2000).
[53] S. A. Bonev, B. Militzer, and G. Galli, Phys. Rev. B **69**, 014101 (2004).
[54] S. Khairallah, J. Shumway, and E. Draeger, arXiv:1108.1711.
[55] M. Knaup, P. Reinhard, C. Toepffer, and G. Zwicknagel, J. Phys. A **36**, 6165 (2003).
[56] J. P. Perdew, K. Burke, and M. Ernzerhof, Phys. Rev. Lett. **77**, 3865 (1996).
[57] G. W. Collins, P. M. Celliers, L. B. Da Silva, R. Cauble, D. M. Gold, M. E. Foord, N. C. Holmes, B. A. Hammel, R. J. Wallace, and A. Ng, Phys. Rev. Lett. **87**, 165504 (2001).
[58] J. E. Bailey, M. D. Knudson, A. L. Carlson, G. S. Dunham, M. P. Desjarlais, D. L. Hanson, and J. R. Asay, Phys. Rev. B **78**, 144107 (2008).
[59] N. C. Holmes, M. Ross, and W. J. Nellis, Phys. Rev. B **52**, 15835 (1995).
[60] W. Nellis, M. Ross, and N. Holmes, Science **269**, 1249 (1995).
[61] S. T. Weir, A. C. Mitchell, and W. J. Nellis, Phys. Rev. Lett. **76**, 1860 (1996).
[62] W. J. Nellis, A. C. Mitchell, M. van Thiel, G. J. Devine, and R. J. Trainor, J. Chem. Phys. **79**, 1480 (1983).
[63] T. Sano, N. Ozaki, T. Sakaiya, K. Shigemori, M. Ikoma, T. Kimura, K. Miyanishi, T. Endo, A. Shiroshita, and H. Takahashi, J. Phys. Conf. Ser. **244**, 042018 (2010).
[64] P. Giannozzi, S. Baroni, N. Bonini, M. Calandra, R. Car, C. Cavazzoni, D. Ceresoli, G. L. Chiarotti, M. Cococcioni, I. Dabo, A. Dal Corso, S. de Gironcoli, S. Fabris, G. Fratesi, R. Gebauer, U. Gerstmann, C. Gougoussis, A. Kokalj, M. Lazzeri, L. Martin-Samos *et al.*, J. Phys. Condens. Matter **21**, 395502 (2009).
[65] M. Holzmann, D. M. Ceperley, C. Pierleoni, and K. Esler, Phys. Rev. E **68**, 046707 (2003).
[66] C. Pierleoni, K. T. Delaney, M. A. Morales, D. M. Ceperley, and M. Holzmann, Comput. Phys. Commun. **179**, 89 (2008).
[67] D. M. Ceperley and B. J. Alder, Phys. Rev. B **36**, 2092 (1987).
[68] D. Ceperley and M. H. Kalos, in *Monte Carlo Methods in Statistical Physics*, edited by K. Binder (Springer-Verlag, New York, 1979), p. 145.
[69] C. Lin, F. H. Zong, and D. M. Ceperley, Phys. Rev. E **64**, 016702 (2001).
[70] S. Chiesa, D. M. Ceperley, R. M. Martin, and M. Holzmann, Phys. Rev. Lett. **97**, 076404 (2006).
[71] N. D. Drummond, R. J. Needs, A. Sorouri, and M. M. C. Foulkes, Phys. Rev. B **78**, 125106 (2008).
[72] See Supplemental Material at http://link.aps.org/supplemental/10.1103/PhysRevLett.115.045301 for detailed information on the finite size effects used in our analysis of the Hugoniot.
[73] R. M. Martin, *Electronic Structure: Basic Theory and Practical Methods* (Cambridge University Press, Cambridge, 2004).
[74] N. D. Mermin, Phys. Rev. **137**, A1441 (1965).
[75] M. Städele and R. M. Martin, Phys. Rev. Lett. **84**, 6070 (2000).
[76] H. Chacham and S. G. Louie, Phys. Rev. Lett. **66**, 64 (1991).
[77] H. Chacham, X. Zhu, and S. G. Louie, Phys. Rev. B **46**, 6688 (1992).
[78] S. Azadi and W. M. C. Foulkes, Phys. Rev. B **88**, 014115 (2013).